

# Modeling Time-Varying Aggregate Interference in Cognitive Radio Systems, and Application to Primary Exclusive Zone Design

Mohd. Shabbir Ali and Neelesh B. Mehta, *Senior Member, IEEE*

**Abstract**—Accurately characterizing the time-varying interference caused to the primary users is essential in ensuring a successful deployment of cognitive radios (CR). We show that the aggregate interference at the primary receiver (PU-Rx) from multiple, randomly located cognitive users (CUs) is well modeled as a shifted lognormal random process, which is more accurate than the lognormal and the Gaussian process models considered in the literature, even for a relatively dense deployment of CUs. It also compares favorably with the asymptotically exact stable and symmetric truncated stable distribution models, except at high CU densities. Our model accounts for the effect of imperfect spectrum sensing, which depends on path-loss, shadowing, and small-scale fading of the link from the primary transmitter to the CU; the interweave and underlay modes of CR operation, which determine the transmit powers of the CUs; and time-correlated shadowing and fading of the links from the CUs to the PU-Rx. It leads to expressions for the probability distribution function, level crossing rate, and average exceedance duration. The impact of cooperative spectrum sensing is also characterized. We validate the model by applying it to redesign the primary exclusive zone to account for the time-varying nature of interference.

**Index Terms**—Cognitive radio, interference, spectrum sensing, underlay, interweave, shadowing, fading, time-variations, random process, lognormal, primary exclusive zone.

## I. INTRODUCTION

COGNITIVE radio (CR) offers a promising solution to the problem of under utilization of the spectrum. A common paradigm of CR classifies users into two categories, namely, primary users (PUs), which have unfettered access to the spectrum, and cognitive users (CUs), which can use the spectrum but under tight constraints on the aggregate interference their transmissions cause to the PUs [1]–[6]. A successful design and deployment of CR, therefore, requires as a first step an accurate model for the aggregate interference caused to the PUs by transmissions from one or many CUs. This characterization feeds into the design and evaluation of transmission policies for the CUs and techniques to help mitigate their interference.

Several factors together affect the aggregate interference, and must be accounted for in order to arrive at an accurate

model for it. It is affected by propagation characteristics of the channels between the CUs and PUs, such as path-loss, shadowing, and fading. Furthermore, the number of CUs that transmit and their locations affect the interference. Imperfect spectrum sensing also directly affects it as it determines the CUs' transmit powers and whether or not they transmit. The use of cooperation, in which the CUs cooperate with each other and fuse their decisions, affects the accuracy of spectrum sensing and, thus, the aggregate interference.

Given the importance of interference modeling in CR, one of the approaches pursued in the literature is based on measurements from test deployments [7]–[9]. However, these deployments are typically small because of the difficulty in setting up an experiment with many interferers that captures the many sources of randomness. Furthermore, the models deduced are location-specific. Therefore, a second approach has focused on developing statistical models for the aggregate interference [1]–[5]. However, no closed form exists for its probability distribution function (PDF). Therefore, several approximate analytical models have been investigated.

*Interference in Underlay CR Mode:* In the underlay mode, a CU can transmit even when it senses that the PU transmitter (PU-Tx) is transmitting [10]. However, it does so with a much lower power in order to avoid excessive interference to the PU receiver (PU-Rx). In [5], the aggregate interference at the PU-Rx from a fixed number of CUs, which are distributed uniformly over a region, is modeled as a lognormal random variable (RV). However, only large-scale shadow fading is taken into account. A spatial Poisson point process (SPPP) model is instead assumed to model the randomness in the CU number and locations in [4], and the aggregate interference is modeled as a lognormal RV. Power control as well as contention control, in which CUs too close to each other do not transmit simultaneously, are accounted for. Furthermore, lognormal shadowing and Nakagami- $m$  fading are modeled. However, imperfect spectrum sensing and the time-varying nature of aggregate interference are not studied in [4], [5].

*Interference in Interweave CR Mode:* In the interweave mode, a CU transmits only when it senses the PU-Tx to be off [10]. The transmission can be in the same band as the PU-Tx or in a different band. In [2], the amplitude of the aggregate interference is modeled as a symmetric truncated-stable (STS) RV. Unlike the stable distribution model [1], the STS model ensures finite second and higher moments. An SPPP model determines the CU locations and an energy detector (ED) is used for spectrum sensing. A detect-and-

Manuscript received April 30, 2013; revised August 6 and October 8, 2013; accepted October 12, 2013. The associate editor coordinating the review of this paper and approving it for publication was R. Zhang.

The authors are with the Dept. of Electrical Communication Eng., Indian Institute of Science (IISc), Bangalore, India (e-mail: mdshabbirali88@gmail.com, nbmehta@ece.iisc.ernet.in).

This work was partially supported by a research grant from ANRC.

A part of the work has been accepted for presentation in the IEEE Global Conf. on Communications (GlobeCom), 2013.

Digital Object Identifier 10.1109/TWC.2013.113013.130762

avoid strategy in which the transmit power level of the CU is adapted based on the received signal strength is considered. Cooperative spectrum sensing is accounted for in [3], which models the aggregate interference as a shifted lognormal (SLN) RV assuming an SPPP model for the CUs. However, time variations are not modeled in [1]–[3].

### A. Contributions

We develop a comprehensive model for the aggregate interference that captures its snapshot statistics, i.e., PDF, as well as its time-variation statistics, which is measured in terms of the auto-correlation function, average level crossing rate (LCR), and average exceedance duration (AED) [11]. We show that the aggregate interference is well modeled as a wide sense stationary (WSS) SLN random process (RP), except when it is small. Our model allows the CUs to operate in both the interweave and underlay modes, in which they transmit in the same band as the PU-Tx with a high power when they sense the PU-Tx to be off and with a low power when they sense the PU-Tx to be on. It accounts for imperfect spectrum sensing, which depends on the location of the CU relative to the PU-Tx. Also, it accounts for the combined effect of time-correlated shadowing and Rayleigh fading on the various links. We also extensively benchmark the proposed model with several other models proposed in the literature. The randomness in the CU locations and number is also captured using the SPPP model.

We then develop a corresponding model for the aggregate interference for cooperative spectrum sensing, in which CUs that are close to each other cooperate and arrive at a common decision. We show that the SLN RP again models the aggregate interference well, except when it is small, and brings out the reduction in the aggregate interference due to cooperation.

We then demonstrate the usefulness and tractability of the proposed model by refining the design of the primary exclusive zone (PEZ) [4], [12], [13]. The PEZ is defined as the region around the PU-Rx within which no CU is allowed to transmit, and helps protect the PU-Rx from excessive interference. Its area affects the aggregate interference experienced by the PU-Rx. We propose a novel criterion for determining the PEZ radius that incorporates the impact of the time-varying nature of the aggregate interference.

### B. Comparisons with Literature

The SLN model has been considered before in the literature [3], [14]. Further, our channel model and the SPPP model for CUs is similar to that in [3]. However, the generalization from an SLN RV to an SLN RP, and the demonstration of its accuracy in modeling the time-varying nature of the aggregate interference when all the aforementioned physical layer effects are accounted for is novel and is a contribution of this paper. The following is a list of our specific contributions and the many ways in which our approach and results differ from those in [3] and other related works [1], [2], [12]–[17]:

- *Overall goal:* While [3] focuses on characterizing the snapshot statistics and models the aggregate interference as an SLN RV, we characterize the time-varying behavior of the aggregate interference as it also affects the PU-Rx. For example, in [15], it has been argued that long dips

in the signal-to-noise-plus-interference-ratio (SINR) are detrimental to the PU-Rx. Our model is also more general than the LCR analysis in [16], which considers a system with one CU and one PU, only models shadowing, and assumes perfect spectrum sensing.

While the stable model is provably accurate in the asymptotic regime of a large number of CUs [1], generalizing it or the STS model to incorporate time-variations is an open problem. These two models also require accurate, numerically stable techniques to compute the cumulative distribution function (CDF) from the characteristic function (CF) that they characterize. Furthermore, as we shall see, the asymptotic exactness manifests itself only at higher CU densities. In [17], the aggregate interference is instead modeled as a gamma RP. However, shadowing and imperfect spectrum sensing are not modeled and the number of CUs is assumed to be fixed. In [14], the SLN RV has instead been used for approximating the decision statistics of a multichannel energy detector. Thus, its model and results are very different from ours.

- *Analytical results:* While moments of the aggregate interference are derived in [3], we derive new expressions for the moments and the autocorrelation of the aggregate interference. These then help determine all the parameters that are required to specify the SLN RP, and beget new analytical results for the LCR and AED of the aggregate interference. Our moment expressions also turn out to be different due to differences in our CU transmission and spectrum sensing models, which are summarized below.
- *CU transmission model:* While [3] focuses on the interweave mode, we analyze a hybrid mode of operation that combines the interweave and underlay modes.
- *Spectrum sensing model:* In [3], an out-of-band spectrum sensing model is assumed in which each CU senses the signal it receives from the full-duplex PU-Rx on a separate control channel. In our model, however, spectrum sensing is based on the signal received from the PU-Tx and is in-band [2], [18]. This also avoids the need for the CUs to simultaneously sense an out-of-band beacon. Another difference, which also affects spectrum sensing, is that we incorporate the PEZ in our model.
- *Extensive benchmarking and application:* Our paper also demonstrates the utility of the proposed RP model by applying it to the design of the PEZ, and showing that it is reasonably accurate over a wide range of parameters. This is unlike [3]. Further, the benchmarking of the proposed model is more extensive in our paper.
- *New PEZ design criteria:* The incorporation of the time-varying nature of the interference in the PEZ design is a contribution of the paper, and has not been considered in [12], [13]. Further [12], did not consider imperfect spectrum sensing, shadowing, and small-scale fading, while imperfect spectrum sensing was not modeled in [13]. Our quantification of how cooperative spectrum sensing shrinks the PEZ is also novel.

The paper is organized as follows. Sec. II describes the system model. The aggregate interference process model is developed in Sec. III. Cooperative spectrum sensing is con-

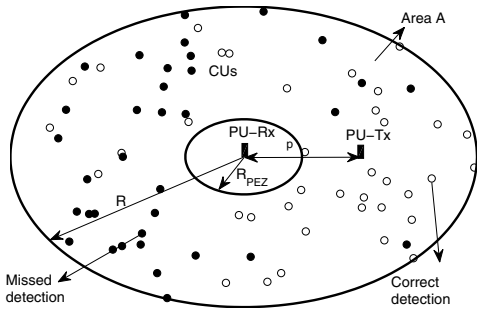


Fig. 1. System model showing the spectrum sensing by the CUs that are scattered over a region of area  $A$ .

sidered in Sec. IV. Simulation results and PEZ redesign are presented in Sec. V. Our conclusions follow in Sec. VI.

## II. SYSTEM MODEL

We shall use the following notation. Expectation is denoted by  $\mathbb{E}[\cdot]$ , and  $\mathbb{E}_X[\cdot]$  denotes expectation conditioned over the RV  $X$ . The notation  $X(t) \sim \mathcal{N}(\mu_X, \sigma_X^2, C_X(\tau))$  shall mean that  $X(t)$  is a WSS Gaussian RP with mean  $\mu_X$ , variance  $\sigma_X^2$ , and covariance function  $C_X(\tau)$ . Similarly,  $X \sim \mathcal{N}(\mu_X, \sigma_X^2)$  denotes a Gaussian RV, and  $X \sim \exp(\mu)$  denotes an exponential RV with mean  $\mu$ .

### A. System Layout

Figure 1 shows the system layout. The number and locations of the CUs is modeled using a homogeneous SPPP, which is characterized by a density parameter  $\Upsilon$ . Therefore, the number of CUs  $N_{CR}$  that occur in a region of area  $A$  is a Poisson RV with mean  $\Upsilon A$ . The PU-Rx is located at the center of the region and the PU-Tx is located at a distance  $p$  from the PU-Rx on the x-axis. The region of radius  $R_{PEZ}$  around the PU-Rx is the PEZ, within which no CU transmits [4], [12], [13]. The PEZ can be constructed using an in-band beacon signal from the PU-Rx or using geo-location [4].<sup>1</sup> Note that this beacon aided model is different from that in [3], in which the CU transmissions are governed by an out-of-band beacon sent by the full-duplex PU-Rx anytime the PU-Tx transmits.

### B. Channel Model

The power  $P_{Ri}(t)$  received at the PU-Rx from the  $i^{\text{th}}$  CU, which is located at a distance  $r_i(t)$  from it, is given by

$$P_{Ri}(t) = PK \left( \frac{d_0}{r_i(t)} \right)^\eta e^{\beta X_i(t)} h_i(t), \quad (1)$$

where  $P$  is the transmit power of the CU. The path-loss component is  $K \left( \frac{d_0}{r_i(t)} \right)^\eta$ , where  $K = \left( \frac{\lambda}{4\pi d_0} \right)^2$ ,  $\lambda$  is the carrier wavelength,  $d_0$  is the break-point distance, and  $\eta$  is the path-loss exponent [11]. The Rayleigh fading component is  $h_i(t) \sim \exp(1)$ . Note that our model can also handle any other

<sup>1</sup>The CUs within the PEZ are all assumed to know that they are within it. This is justified because several measurements of the PU-Rx beacon collected over a sufficiently long duration of time can be used to ensure this.

mean for  $h_i(t)$ . The normalized covariance function  $C_{h_i}(\tau)$  is given as per the Jakes' fading model [11]:

$$C_{h_i}(\tau) = J_0^2(2\pi f_m \tau), \quad (2)$$

where  $f_m$  is the maximum Doppler spread and  $J_0$  is the Bessel function of first kind of order zero [19]. The shadowing component is  $e^{\beta X_i(t)}$ , where  $\beta = \frac{\log 10}{10}$  and  $X_i(t) \sim \mathcal{N}(0, \sigma_{sh}^2, C_{X_i}(\tau))$ . The covariance function  $C_{X_i}(\tau)$  is given by the modified Gudmundson's model as [15]

$$C_{X_i}(\tau) = \sigma_{sh}^2 \exp\left(-\frac{v^2 \tau^2}{2D^2}\right), \quad (3)$$

where  $v$  is the speed of the CU and  $D$  is the decorrelation distance. The shadowing and fading seen by different CUs on their links from the PU-Tx and to the PU-Rx are independent and identically distributed (IID).

### C. PU-Tx Based Spectrum Sensing (SS)

The accuracy of SS by the CU depends on the strength of the signal it receives from the PU-Tx and the SS algorithm used. We consider the popular ED-based SS algorithm [20] assuming that all the CUs periodically spectrum sense together for a short duration.<sup>2</sup> In [20], the SS algorithm declares the PU-Tx to be on if the energy received by the CU from it over a time  $T$  and bandwidth  $B$  exceeds a threshold  $\xi$ .

For this detector, the false alarm probability  $P_{FA}$  at the  $i^{\text{th}}$  CU is  $Q\left(\frac{\xi - N_0 T B}{N_0^2 T B}\right)$ , where  $N_0$  is the noise power and  $Q$  is the Gaussian  $Q$  function. The correct detection probability depends on the signal-to-noise-ratio (SNR)  $\gamma(\Delta_i, Y_i, g_i)$  of the PU-Tx signal at the CU, which in turn depends on the distance  $\Delta_i$  of the CU from the PU-Tx, shadowing  $e^{\beta Y_i}$ , and Rayleigh fading  $g_i$  during the time of sensing. Here,  $Y_i \sim \mathcal{N}(0, \sigma_{sh}^2)$  and  $g_i \sim \exp(1)$ . The expression for the correct detection probability, denoted by  $P_D(\Delta_i, Y_i, g_i)$ , in terms of  $P_{FA}$  is [20]

$$P_D(\Delta_i, Y_i, g_i) = Q\left(\frac{Q^{-1}(P_{FA}) - \gamma(\Delta_i, Y_i, g_i) \sqrt{TB}}{\sqrt{1 + 2\gamma(\Delta_i, Y_i, g_i)}}\right). \quad (4)$$

Note that our model can include other SS algorithms as well, e.g., [22]; the expressions for  $P_{FA}$  and  $P_D$  will differ.

### D. CU Transmission and Interference Model

If a CU detects the PU-Tx to be on, which we refer to as hypothesis  $H_1$ , then it operates in the underlay mode and transmits with a lower power  $P_u$ . Else, if the CU detects the PU-Tx to be off, which we refer to as hypothesis  $H_0$ , then it operates in the interweave mode and transmits with a higher power  $P_o$ . In both cases, it transmits in the same band as the PU-Tx. Therefore, from (1), the interference power  $I_i(t)$  at the PU-Rx from the  $i^{\text{th}}$  CU, which is  $r_i(t)$  distance away, is

$$I_i(t) = \begin{cases} P_u K \left( \frac{d_0}{r_i(t)} \right)^\eta e^{\beta X_i(t)} h_i(t), & \text{if } H_1 \text{ is detected,} \\ P_o K \left( \frac{d_0}{r_i(t)} \right)^\eta e^{\beta X_i(t)} h_i(t), & \text{if } H_0 \text{ is detected.} \end{cases} \quad (5)$$

<sup>2</sup>If the CUs sense the spectrum asynchronously then the aggregate interference from the concurrent transmissions by other CUs has to be taken into account along the lines of [21].

Note that this two-level transmit power model may not be the most suitable one in the presence of interference from other systems. One possible way to improve it is to use the more advanced detect-and-avoid strategy [2]. Further, energy detection might no longer be the right SS method to use since it cannot differentiate between the sources of interference.

### III. INTERFERENCE MODELING: NON-COOPERATIVE SS

The aggregate interference  $I_\Sigma(t)$  at the PU-Rx from the CUs is

$$I_\Sigma(t) = \sum_{i=1}^{N_{CR}} I_i(t). \quad (6)$$

Our goal is to accurately model the time evolution of  $I_\Sigma(t)$  in between the SS durations when the PU-Tx is on. We now develop the moment-matching-based WSS SLN RP model, as per which  $I_\Sigma(t)$  is modeled as

$$I_\Sigma(t) \approx e^{Z(t)} + s, \quad (7)$$

where  $Z(t) \sim \mathcal{N}(\mu_Z, \sigma_Z^2, C_Z(\tau))$  and  $s$  is called the *shift parameter*. Our goal is to determine the constants  $\mu_Z$ ,  $\sigma_Z$ , and  $s$ , and  $C_Z(\tau)$  by matching them with the corresponding terms of  $I_\Sigma(t)$ . To do so, we first express these parameters in terms of the cumulants of  $I_\Sigma(t)$ . The cumulants are then written in terms of  $\mathbb{E}[I_i(t)^m]$ , for  $m = 1, 2, 3$ , and  $\mathbb{E}[I_i(t)I_i(t + \tau)]$ , which are derived in Results 1 and 2. It is here that the main contribution of this section lies.

In terms of the cumulants of  $I_\Sigma(t)$ , the parameters  $\mu_Z$ ,  $\sigma_Z$ , and  $s$  are given by [14]

$$\sigma_Z^2 = \log\left(\frac{1}{4}\Psi^{\frac{2}{3}} + 4\Psi^{-\frac{2}{3}} - 1\right), \quad (8)$$

$$\mu_Z = \frac{1}{2} \log\left(\frac{\kappa_{I_\Sigma}(2)}{e^{\sigma_Z^2} - 1}\right) - \frac{1}{2}\sigma_Z^2, \quad (9)$$

$$s = \kappa_{I_\Sigma}(1) - \exp\left(\mu_Z + \frac{1}{2}\sigma_Z^2\right), \quad (10)$$

where  $\Psi = 4\kappa_{I_\Sigma}(3) + 4\sqrt{4 + (\kappa_{I_\Sigma}(3))^2}$  and  $\kappa_{I_\Sigma}(m)$  is the  $m^{\text{th}}$  cumulant of  $I_\Sigma(t)$ , which is defined as [19, (26.1.12)]

$$\begin{aligned} \kappa_{I_\Sigma}(m) &= \frac{1}{j^m} \frac{d^m \log\left(\mathbb{E}\left[e^{j\omega I_\Sigma(t)}\right]\right)}{d\omega^m} \Bigg|_{\omega=0}, \\ &= \frac{1}{j^m} \frac{d^m \log\left(\mathbb{E}_{N_{CR}}\left[\left(\mathbb{E}\left[e^{j\omega I_i(t)}\right]\right)^{N_{CR}}\right]\right)}{d\omega^m} \Bigg|_{\omega=0}, \end{aligned} \quad (11)$$

where  $j = \sqrt{-1}$ . The second equality is obtained by using (6), conditioning on  $N_{CR}$ , and using the fact that all  $I_i(t)$ , for  $1 \leq i \leq N_{CR}$ , are IID for the SPPP that governs the locations of the CUs. Upon taking the expectation over  $N_{CR}$  and then evaluating the derivative, we get

$$\kappa_{I_\Sigma}(m) = \pi \left(R^2 - R_{\text{PEZ}}^2\right) \Upsilon \mathbb{E}[I_i(t)^m]. \quad (12)$$

The SLN RP model also requires  $C_Z(\tau)$ . As shown in Appendix A, it is equal to

$$\begin{aligned} C_Z(\tau) &= \log\left(\pi \left(R^2 - R_{\text{PEZ}}^2\right) \Upsilon \mathbb{E}[I_i(t)I_i(t + \tau)]\right) \\ &\quad + e^{2\mu_Z + \sigma_Z^2} - (2\mu_Z + \sigma_Z^2). \end{aligned} \quad (13)$$

#### A. With Path-loss and Shadowing

We first analyze the case when small-scale fading is averaged out. This is of interest when the PU-Rx can average over the fast variations of the small-scale fading [11, Chap. 3].

The distance  $q(r_i(t), p, \cos \theta_i)$  between the PU-Tx and the  $i^{\text{th}}$  CU is equal to

$$q(r_i(t), p, \cos \theta_i) = \sqrt{r_i(t)^2 + p^2 - 2r_i(t)p \cos \theta_i}, \quad (14)$$

where  $\theta_i$  is the azimuth angle of the CU. The PDF  $p_{\theta_i}$  of  $\theta_i$  and the PDF  $p_{r_i}$  of  $r_i(t)$ , conditioned on the CU not lying in the PEZ, are given by

$$\begin{aligned} p_{\theta_i}(x) &= \frac{1}{2\pi}, \quad 0 \leq x < 2\pi, \\ p_{r_i}(x) &= \frac{2x}{R^2 - R_{\text{PEZ}}^2}, \quad R_{\text{PEZ}} \leq x < R. \end{aligned} \quad (15)$$

**Result 1:** The  $m^{\text{th}}$  moment of the interference from an arbitrary CU  $i$  is then given by

$$\begin{aligned} \mathbb{E}[I_i(t)^m] &\approx \frac{2P_o^m K^m d_0^{m\eta} \left(R_{\text{PEZ}}^{2-m\eta} - R^{2-m\eta}\right)}{(m\eta - 2)(R^2 - R_{\text{PEZ}}^2)} e^{\frac{1}{2}m^2\beta^2\sigma_{\text{sh}}^2} \\ &\quad - \frac{2(P_o^m - P_u^m) K^m}{\sqrt{\pi}W_c(R^2 - R_{\text{PEZ}}^2)} e^{\frac{1}{2}m^2\beta^2\sigma_{\text{sh}}^2} \\ &\quad \times \sum_{n_1=1}^{W_h} w_h(n_1) \sum_{n_2=1}^{W_l} w_l(n_2) \sum_{n_3=1}^{W_c} \int_{R_{\text{PEZ}}}^R \frac{d_0^{m\eta}}{r_i^{m\eta-1}} \\ &\quad \times P_D\left(q(r_i, p, a_c(n_3)), \sqrt{2}\sigma_{\text{sh}}a_h(n_1), a_l(n_2)\right) dr_i. \end{aligned} \quad (16)$$

*Proof:* The proof is given in Appendix B. ■

Here,  $w_h(n)$  and  $a_h(n)$ , for  $n = 1, \dots, W_h$ , denote the weights and the abscissas, respectively, of Gauss-Hermite quadrature,  $a_c(n)$ , for  $n = 1, \dots, W_c$ , denote the abscissas of Gauss-Chebyshev quadrature, and  $w_l(n)$  and  $a_l(n)$ , for  $n = 1, \dots, W_l$ , denote the weights and the abscissas, respectively, of Gauss-Laguerre quadrature [19, (25.4.38), (25.4.45), (25.4.46)].

**Result 2:** The auto-correlation of the interference from a CU is given as follows:

$$\begin{aligned} \mathbb{E}[I_i(t)I_i(t + \tau)] &\approx \frac{P_o^2 K^2 d_0^{2\eta} \left(R_{\text{PEZ}}^{2-2\eta} - R^{2-2\eta}\right)}{(\eta - 1)(R^2 - R_{\text{PEZ}}^2)} \\ &\quad \times e^{\beta^2\sigma_{\text{sh}}^2 \left(1 + \exp\left(-\frac{v^2\tau^2}{2D^2}\right)\right)} - \frac{2(P_o^2 - P_u^2)K^2}{\sqrt{\pi}W_c(R^2 - R_{\text{PEZ}}^2)} \\ &\quad \times e^{\beta^2\sigma_{\text{sh}}^2 \left(1 + \exp\left(-\frac{v^2\tau^2}{2D^2}\right)\right)} \sum_{n_1=1}^{W_h} w_h(n_1) \sum_{n_2=1}^{W_l} w_l(n_2) \sum_{n_3=1}^{W_c} \\ &\quad \int_{R_{\text{PEZ}}}^R \frac{d_0^{2\eta}}{r_i^{2\eta-1}} P_D\left(q(r_i, p, a_c(n_3)), \sqrt{2}\sigma_{\text{sh}}a_h(n_1), a_l(n_2)\right) dr_i. \end{aligned} \quad (17)$$

*Proof:* The proof is given in Appendix C. ■

The final expressions in (16) and (17) are in the form of single integrals. These cannot be simplified further because of the presence of the  $P_D$  term inside the integrand, which depends on the SS algorithm. It is typically quite involved, as can be seen from (4). The integrals are easily evaluated numerically. In general, as the number of the Gauss-quadrature

terms increases, the error between the integral and the approximating sum decreases [19, (25.4.38),(25.4.45),(25.4.46)]. We have found that for our problem  $W_h = W_c = W_l = 6$  is sufficient to ensure accurate complementary CDF (CCDF) and LCR curves for  $\sigma_{sh} \leq 12$ .

Note that the analysis can be extended to the case where PU-Rx is not at the center of the region. In this case, the distance between the  $i^{\text{th}}$  CU and the PU-Rx, which arises in (5), changes. However, the expressions of the moments and the auto-correlation of  $I_i(t)$  can still be obtained in a single integral form. The case where the distance  $p$  between the PU-Rx and PU-Tx is an RV can also be incorporated. In this case, an additional expectation over  $p$  will appear in (16) and (17).

### B. With Path-loss, Shadowing, and Fading

If the PU-Rx cannot average over the small-scale fading, then this should be taken into account in the aggregate interference model. When small-scale fading is also considered along with path-loss and shadowing, the expression for the  $m^{\text{th}}$  moment  $\mathbb{E}[I_i(t)^m]$  in (32) will get multiplied by a factor  $\mathbb{E}[h_i(t)^m]$ . Using  $\mathbb{E}[h_i(t)^m] = m!$ , and simplifying further yields the expressions for moments that contain an additional factor of  $m!$  compared to (16). Similarly, the auto-correlation  $\mathbb{E}[I_i(t)I_i(t+\tau)]$  in (35) will get multiplied by a factor  $\mathbb{E}[h_i(t)h_i(t+\tau)]$ . Consequently, from (2), the autocorrelation in (17) gets scaled by a factor  $(J_0^2(2\pi f_m \tau) + 1)$ .

### C. CCDF, LCR, and AED of $I_{\Sigma}(t)$ Based on SLN RP Model

For a threshold  $I_{th}$ , the CCDF of  $I_{\Sigma}(t)$  is given by [3, (23)]:  $\Pr(I_{\Sigma}(t) \geq I_{th}) = Q\left(\frac{\log(I_{th}-s)-\mu_Z}{\sigma_Z}\right)$ . The LCR  $L_{I_{\Sigma}(t)}(I_{th})$  of  $I_{\Sigma}(t)$  can be obtained from the level crossing theory of Gaussian processes [23], the key steps for which are shown below. From [23, Lemma 10.2], the LCR can be written in terms of  $Z(t)$  as

$$L_{I_{\Sigma}(t)}(I_{th}) = \lim_{n \rightarrow \infty} \left[ \sum_{i=1}^n \Pr\left(Z\left(\frac{i-1}{n}\right) < \log(I_{th}-s) < Z\left(\frac{i}{n}\right)\right) \right]. \quad (18)$$

Using [23, Theorem 10.1], we then get

$$L_{I_{\Sigma}(t)}(I_{th}) = \frac{\sqrt{\Omega_Z}}{2\pi\sigma_Z} \exp\left(-\frac{(\log(I_{th}-s)-\mu_Z)^2}{2\sigma_Z^2}\right), \quad I_{th} > s, \quad (19)$$

where  $\Omega_Z = -\frac{d^2}{d\tau^2} C_Z(\tau)\Big|_{\tau=0}$  is computed from (13) and (17). Finally, the AED  $\Psi_{I_{\Sigma}(t)}(I_{th})$  of  $I_{\Sigma}(t)$  is the ratio of the CCDF and the LCR:

$$\Psi_{I_{\Sigma}(t)}(I_{th}) = \frac{\Pr(I_{\Sigma}(t) \geq I_{th})}{L_{I_{\Sigma}(t)}(I_{th})}. \quad (20)$$

## IV. INTERFERENCE MODELING: COOPERATIVE SS

We now incorporate cooperative SS into our model, and characterize how it affects the aggregate interference RP. For this purpose, we use the OR fusion rule because it is more preferable than the AND and majority rules from the point of view of protecting the PU-Rx from excessive interference [3].

In it, a CU that has detected the PU-Tx to be on will broadcast its decision to the CUs that lie within a cooperation region of radius  $R_C$  around it. All these CUs will take a logical OR with their decision, which means that they will also then assume that the PU-Tx is on. This is a one shot process – the CUs do not broadcast their decisions yet again. We assume that the interference caused by the short transmissions of the CUs for enabling cooperative SS is negligible. Furthermore, the communication is assumed to be error-free. This is justifiable since only one bit of information needs to be communicated, and can be sent with sufficient protection.

Note that the interference from the CUs will be correlated because their decisions are correlated due to cooperation. To make the analysis tractable, we use a decoupling approximation, in which the interferences from the CUs are assumed to be uncorrelated, but the effect of correlation in their decisions is captured in the probability of correct decision. Such a decoupling approximation has been used to good effect in analyzing wireless local area networks [24]. With this, the expressions for the parameters of the SLN RP model of the aggregate interference with cooperative SS are given by (8), (9), (10), and (13).

As before, to characterize the aggregate interference with cooperative SS, we need the expressions for  $\mathbb{E}[I_i(t)^m]$  and  $\mathbb{E}[I_i(t)I_i(t+\tau)]$ . These are given below when path-loss and shadowing are considered. The distance between the PU-Tx and the  $j^{\text{th}}$  CU that is located within the cooperation range of the  $i^{\text{th}}$  CU is  $q(r_{ij}(t), q(r_i(t), p, \cos\theta_i), \cos\theta_{ij}))$ , which is given by (14), where  $r_{ij}(t)$  is the distance between the  $i^{\text{th}}$  and  $j^{\text{th}}$  CUs, and  $\theta_{ij}$  is the angle subtended by the lines from the  $j^{\text{th}}$  CU and the PU-Tx to the  $i^{\text{th}}$  CU.

**Result 3:** The  $m^{\text{th}}$  moment of interference  $\mathbb{E}[I_i(t)^m]$  from the  $i^{\text{th}}$  CU with cooperative SS is then given by

$$\begin{aligned} \mathbb{E}[I_i(t)^m] &\approx \frac{2P_o^m K^m d_0^{m\eta} (R_{PEZ}^{2-m\eta} - R^{2-m\eta})}{(m\eta - 2)(R^2 - R_{PEZ}^2)} e^{\frac{1}{2}m^2\beta^2\sigma_{sh}^2} \\ &\quad - \frac{2(P_o^m - P_u^m) K^m}{W_c (R^2 - R_{PEZ}^2)} e^{\frac{1}{2}m^2\beta^2\sigma_{sh}^2} \sum_{n_4=1}^{W_c} \int_{R_{PEZ}}^R \frac{d_0^{m\eta}}{r_i^{m\eta-1}} \\ &\quad \times \left(1 - \frac{1-f_1(r_i, a_c(n_4))}{1-f_2(r_i, a_c(n_4))} e^{-\gamma\pi R_c^2 f_2(r_i, a_c(n_4))}\right) dr_i, \quad (21) \end{aligned}$$

where

$$\begin{aligned} f_1(r_i, a_c(n_4)) &= \sum_{n_1=1}^{W_h} \frac{w_h(n_1)}{\sqrt{\pi}} \sum_{n_2=1}^{W_l} w_l(n_2) \\ &\quad \times P_D\left(q(r_i, p, a_c(n_4)), \sqrt{2}\sigma_{sh}a_h(n_1), a_l(n_2)\right), \quad (22) \end{aligned}$$

$$\begin{aligned} f_2(r_i, a_c(n_4)) &= \frac{2}{\sqrt{\pi}W_c R_c^2} \sum_{n_1=1}^{W_h} w_h(n_1) \sum_{n_2=1}^{W_l} w_l(n_2) \\ &\quad \times \sum_{n_3=1}^{W_c} \int_0^{R_C} P_D\left(q(r_{ij}, q(r_i, p, a_c(n_4)), a_c(n_3)), \right. \\ &\quad \left. \sqrt{2}\sigma_{sh}a_h(n_1), a_l(n_2)\right) r_{ij} dr_{ij}. \quad (23) \end{aligned}$$

TABLE I  
SIMULATION PARAMETERS

Parameter	Variable	Value
Transmit power of PU-Tx	$P_{Tx}$	10 dBm
Transmit power of CU in interweave mode	$P_o$	2 dBm
Transmit power of CU in underlay mode	$P_u$	-6 dBm
Noise power	$N_0$	-100 dBm
Density of CUs	$\Upsilon$	100 CUs/km <sup>2</sup>
System bandwidth	$B$	1 MHz
Carrier frequency	$f_c$	900 MHz
Radius of region considered	$R$	1000 m
Radius of PEZ	$R_{PEZ}$	200 m
Distance between PU-Tx and PU-Rx	$p$	500 m
Path-loss exponent	$\eta$	4
Standard deviation of shadow fading	$\sigma_{sh}$	6
Break-point distance	$d_0$	10 m
Speed of CUs	$v$	5 ms <sup>-1</sup>
False alarm probability	$P_{FA}$	10%
Spectrum sensing duration	$T$	50 $\mu$ sec

The auto-correlation  $\mathbb{E}[I_i(t)I_i(t+\tau)]$  is given by

$$\begin{aligned} \mathbb{E}[I_i(t)I_i(t+\tau)] &\approx \frac{P_o^2 K^2 d_0^{2\eta} (R_{PEZ}^{2-2\eta} - R^{2-2\eta})}{(\eta-1)(R^2 - R_{PEZ}^2)} \\ &\times e^{\beta^2 \sigma_{sh}^2 (1 + \exp(-\frac{v^2 \tau^2}{2D^2}))} - \frac{2(P_o^2 - P_u^2) K^2}{W_c (R^2 - R_{PEZ}^2)} \\ &\times e^{\beta^2 \sigma_{sh}^2 (1 + \exp(-\frac{v^2 \tau^2}{2D^2}))} \sum_{n_4=1}^{W_c} \int_{R_{PEZ}}^R \frac{d_0^{2\eta}}{r_i^{2\eta-1}} \\ &\times \left( 1 - \frac{1 - f_1(r_i, a_c(n_4))}{1 - f_2(r_i, a_c(n_4))} e^{-\Upsilon \pi R_C^2 f_2(r_i, a_c(n_4))} \right) dr_i. \quad (24) \end{aligned}$$

*Proof:* The proof is given in Appendix D. ■

Compared to the expressions for the  $m^{\text{th}}$  moment and auto-correlation in Sec. III-A, the  $P_D$  term is different and the moments now depend on the cooperation range  $R_C$ .

As before, when Rayleigh fading is also accounted for, the expression for  $\mathbb{E}[I_i(t)^m]$  in (21) will get scaled by a factor  $m!$ . The expression for  $\mathbb{E}[I_i(t)I_i(t+\tau)]$  in (24) will get scaled by a factor  $(J_0^2(2\pi f_m \tau) + 1)$ .

## V. NUMERICAL RESULTS

We now verify our analysis using Monte Carlo simulations. The parameters used are listed in Table I. The simulations make measurements over up to  $10^5$  drops. In each drop, a random number of CUs and their locations are generated as per the SPPP. Each CU moves with a fixed speed  $v$  in a randomly chosen direction. Every CU performs SS as per Sec. II-C, in case of non-cooperative SS, and as per Sec. IV, in case of cooperative SS. The aggregate interference  $I_\Sigma(t)$  from all the CUs at the PU-Rx is then measured.

We first present results for non-cooperative SS and then for cooperative SS. In each case, we show results for the snapshot statistics and then for the time-varying behavior. For snapshot statistics, we compare the CDF and the CCDF of the various models, as has been done in [2]–[5], [25], [26]. The CDF evaluates the accuracy in matching smaller aggregate interference values, while the CCDF evaluates the accuracy in matching larger aggregate interference values, where the CDF saturates to unity. To compare the accuracy in modeling the

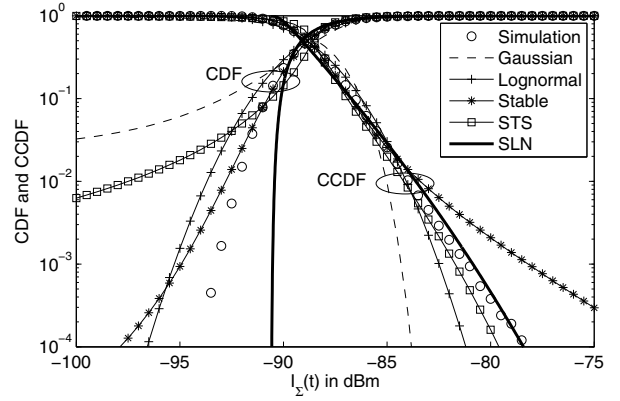


Fig. 2. Non-cooperative SS: Comparison of CDF and CCDF of  $I_\Sigma(t)$  from various models with path-loss and shadowing.

time-variation of the aggregate interference, we study the LCR of the various models, as has been done in [16], [17], [27].

### A. Benchmarking

We compare the SLN model with the following:

- *Gaussian model:* This model is motivated by the central limit theorem. In it,  $I_\Sigma(t)$  is modeled as a Gaussian RP.
- *Lognormal model:* In this model,  $\log(I_\Sigma(t))$  is modeled as a Gaussian RP, along lines similar to [27].
- *STS model:* In this model, the amplitude of  $I_\Sigma(t)$  is modeled as an STS RV [2]. The parameters that determine its CF are obtained by matching the first, second, and fourth cumulants of the STS RV with the corresponding cumulants of the amplitude of  $I_\Sigma(t)$ . The CF is numerically integrated to get the CDF, as closed-form expressions for the latter are not known. Finally, the CDF of  $I_\Sigma(t)$  is determined using a variable transformation.
- *Stable distribution model:* In this model,  $I_\Sigma(t)$  is modeled as stable RV [1]. The parameters that determine the CF are obtained from simulations using the method presented in [28]. The CDF of  $I_\Sigma(t)$  is then obtained by numerically integrating the CF, as a closed-form expression for it is not known.

### B. Non-cooperative SS: With Path-loss and Shadowing

1) *Snapshot Statistics Comparisons:* Figure 2 compares the CDF and the CCDF of the various models when small-scale fading is averaged out. For lower values of aggregate interference ( $I_\Sigma(t) < -90$  dBm), the SLN model underestimates the CDF. However, none of the models proposed in the literature are accurate in this regime.<sup>3</sup> One reason behind this inaccuracy is the use of the moment-matching method, which penalizes less the approximation errors for lower values of interference than for higher values of the interference [26]. Another reason is that the probability that  $I_\Sigma(t)$  is less than  $s$  is zero in the SLN model. For moderate to high values of the aggregate interference ( $I_\Sigma(t) > -90$  dBm), the SLN model matches the

<sup>3</sup>Since the lognormal model overestimates the CDF while the SLN model underestimates it, better accuracy can be achieved by a mixture model whose CDF is the arithmetic mean of the CDFs of these two models [29].

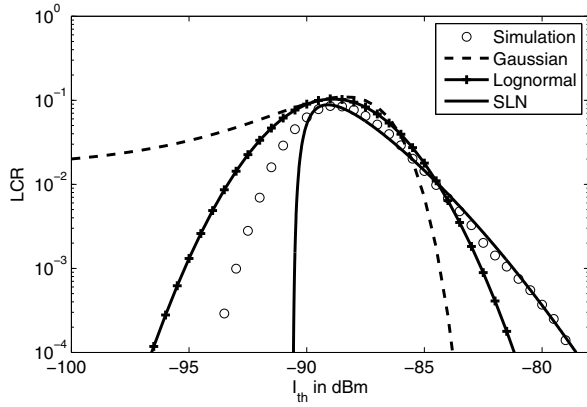


Fig. 3. Non-cooperative SS: Comparison of LCR of  $I_{\Sigma}(t)$  from various models with path-loss and shadowing.

CCDF well and is more accurate than all the other models. It captures the skewness of the interference distribution better than the other models [3]. Note that the  $-90$  dBm value above arises due to the particular choice of simulation parameters. In general, it increases as the mean of the aggregate interference increases.

We see that the Gaussian and lognormal models fail to provide a good fit. For small values of the interference, the CDF of the Gaussian model saturates at  $Q\left(\frac{\mu_G}{\sigma_G}\right)$ , where  $\mu_G$  is the mean and  $\sigma_G^2$  is the variance. Intuitively, this failure is because the rate of convergence of the sum of lognormal RVs is very slow, which is due to the skewed nature of the lognormal PDF [30]. The stable distribution model is better in matching the CDF. However, it gives a poor CCDF match for higher values of the aggregate interference. The STS model matches the CCDF better but its CDF saturates for small values, as was the case with the Gaussian model.

2) *Time-varying Behavior Comparisons:* The LCR of the SLN RP model and the benchmark models is shown in Fig. 3. We see that the LCR curve is not symmetric about the mean of the aggregate interference, which is because the PDF of the aggregate interference is asymmetric about its mean [3]. For low threshold values, the LCR is small because the aggregate interference mostly stays above it and seldom crosses the threshold. As the threshold increases, the LCR increases and reaches a maximum value, which depends on the speed of the CUs. However, as the threshold increases further, the LCR again starts decreasing because the interference is less likely to be high enough to cross it. We again see that the Gaussian RP model is quite inaccurate for both small and large values of interference. For  $I_{th} < -90$  dBm, the lognormal RP model overestimates the LCR while the SLN RP model underestimates it, which is in line with Fig. 2. For  $I_{th} > -90$  dBm, the SLN RP model matches the LCR accurately, and is the most accurate model. As mentioned earlier, corresponding results for the STS model and the stable distribution model are not shown because a time-varying model for them is not known. In both figures, for a CU density of  $\Upsilon = 100$  CUs/km<sup>2</sup>, the average number of CUs in the entire annular region is 302. As the CU density increases and exceeds 500 CUs/km<sup>2</sup>, the proposed model does become more inaccurate.

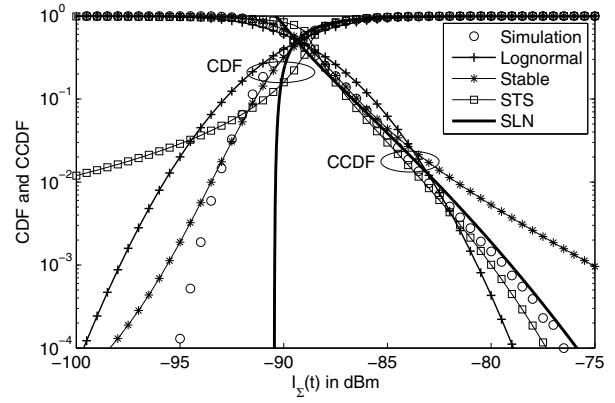


Fig. 4. Non-cooperative SS: Comparison of CDF and CCDF of  $I_{\Sigma}(t)$  from various models with path-loss, shadowing, and Rayleigh fading.

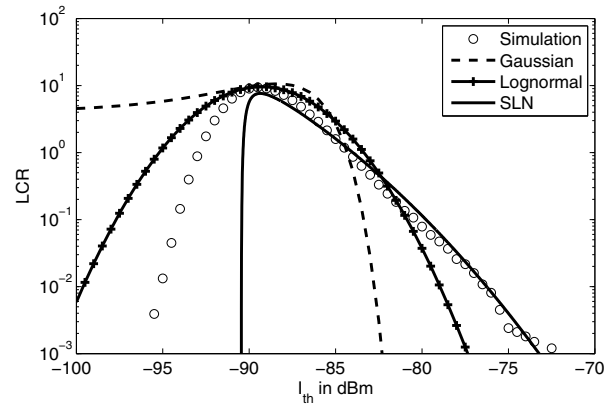


Fig. 5. Non-cooperative SS: Comparison of LCR of  $I_{\Sigma}(t)$  from various models with path-loss, shadowing, and Rayleigh fading.

### C. Non-cooperative SS: Path-loss, Shadowing, and Fading

1) *Snapshot Statistics:* Figure 4 compares the CDF and the CCDF obtained using the various models. To avoid clutter, we do not show the Gaussian model curves as they are quite inaccurate. The observations for the stable and the STS models are qualitatively similar to those in Fig. 2. However, compared to Fig. 2, the CCDF curve shifts to the right due to the additional fluctuations induced by fading. Again, the SLN model matches the CCDF well and is more accurate than the other models.

2) *Time-varying Behavior:* The LCR with both shadowing and Rayleigh fading is shown in Fig. 5. The trends are similar to Fig. 3. However, one important difference is that the maximum value of LCR is 100 times higher than in Fig. 3. This is because of the faster fluctuations due to small-scale fading. For  $I_{th} < -90$  dBm, the lognormal RP model overestimates the LCR whereas the SLN RP model underestimates it, which is in line with Fig. 4. For  $I_{th} > -90$  dBm, the SLN RP model matches the LCR accurately, and is the most accurate model.

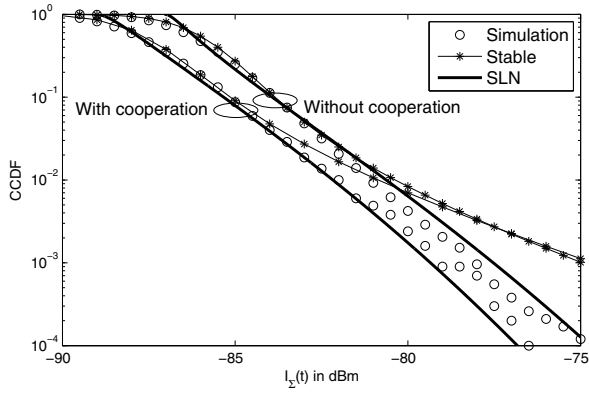


Fig. 6. Comparison of CCDF of  $I_{\Sigma}(t)$  with non-cooperative and cooperative SS from various models with shadowing and Rayleigh fading ( $\Upsilon = 200$  CUs/km<sup>2</sup> and  $R_C = 100$  m).

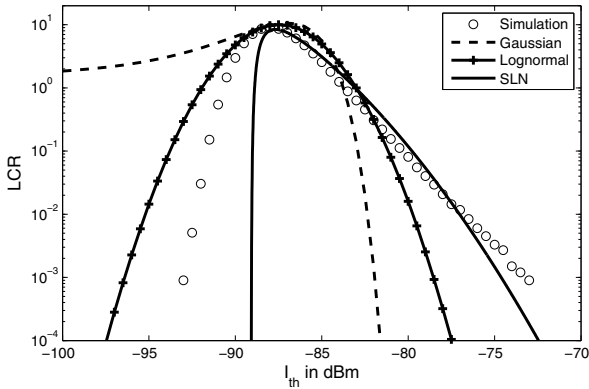


Fig. 7. Cooperative SS: Comparison of LCR of  $I_{\Sigma}(t)$  from various models with shadowing and Rayleigh fading ( $\Upsilon = 200$  CUs/km<sup>2</sup> and  $R_C = 100$  m).

#### D. Cooperative SS: With path-loss, Shadowing, and Fading

1) *Snapshot Statistics*: Figure 6 compares the CCDF of  $I_{\Sigma}(t)$  using the stable and SLN models with cooperative and non-cooperative SS. A CU density of 200 CUs/km<sup>2</sup> and a cooperation range of  $R_C = 100$  m are considered. The Gaussian, lognormal, and STS models are not shown to avoid clutter. The stable model's CCDF deviates from the simulations for higher values of the interference. We again see that the SLN model provides an accurate match.

We also see in Fig. 6 that the CCDF of the aggregate interference with cooperation is 2 dB to the left of the CCDF without cooperation. This is because the aggregate interference has decreased. In general, as  $R_C$  increases, more CUs will cooperate, detect the PU-Tx to be on, and transmit with low power. This reduces the aggregate interference.

2) *Time-varying Behavior*: The LCR of the aggregate interference with cooperative SS is shown in Fig. 7 for the Gaussian, lognormal, and SLN RP models. The SLN model matches the LCR for higher values of the interference better than the other models. The Gaussian model is again the least accurate. For  $I_{th} < -90$  dBm, the lognormal model overestimates the LCR, and for higher values of interference, it underestimates the LCR.

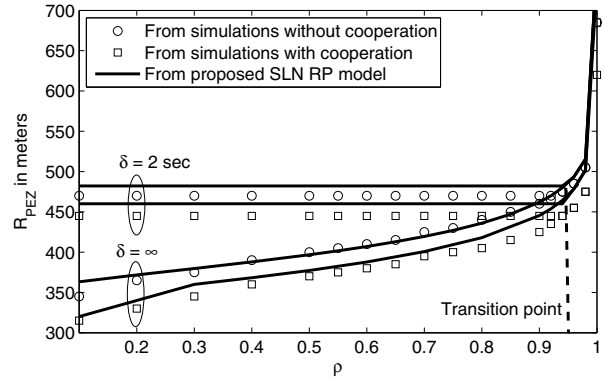


Fig. 8. Zoomed-in view of PEZ radius as a function of  $\rho$  using the SLN model with path-loss and shadowing. Results for non-cooperative and cooperative SS are compared ( $\Upsilon = 100$  CUs/km<sup>2</sup>,  $R_C = 100$  m, and  $I_{th} = -95$  dBm). The transition point shows the value of  $\rho$  below which the AED constraint is active.

#### E. Application to PEZ Design

We now apply the analytical model for aggregate interference to redesign the PEZ based on two constraints. The first constraint is the classical outage probability constraint, which mandates that the probability that the aggregate interference  $I_{\Sigma}(t)$  is greater than a threshold  $I_{th}$  should not exceed  $(1 - \rho)$  [3]. The second constraint is the outage duration constraint, which is new. It is motivated by the minimum outage duration concept [15]. It mandates that the average time duration for which  $I_{\Sigma}(t)$  remains above  $I_{th}$  should not exceed  $\delta$ . An alternate approach is to cast the above constraints in terms of the SINR of the PU, as has been done in [5]. However, the analysis is more involved.

Figure 8 plots  $R_{PEZ}$  as a function of  $\rho$  for different values of  $\delta$  with only path-loss and shadowing. Figure 9 plots the corresponding results with path-loss, shadowing, and fading. Results obtained by using the formulae developed for the SLN model are compared with those obtained from an extensive Monte Carlo simulation-based search. In both figures, results are shown for both non-cooperative and cooperative SS. The  $\delta = \infty$  case corresponds to only the outage constraint being active. Observe the good agreement between the simulation results and the results obtained using the SLN model. As  $\rho$  increases, the outage constraint becomes tighter and  $R_{PEZ}$  increases. Furthermore, cooperation shrinks  $R_{PEZ}$ , which means that more CUs can transmit closer to the PU-Rx without excessively interfering with it. For  $\delta = 2$  sec in Fig. 8 and  $\delta = 30$  msec in Fig. 9, the AED constraint is active for  $\rho < 0.95$  and  $\rho < 0.86$ , respectively. Thus, the AED constraint is active for a large range of values of  $\rho$  with and without cooperative SS.

## VI. CONCLUSIONS

We characterized the aggregate interference caused by CUs, which transmit with different powers depending on whether they sense the PU-Tx to be on or off. Our model accounted for the dependence of the aggregate interference on the random locations and number of the CUs, their imperfect spectrum sensing, and the time-varying nature of large-scale shadowing

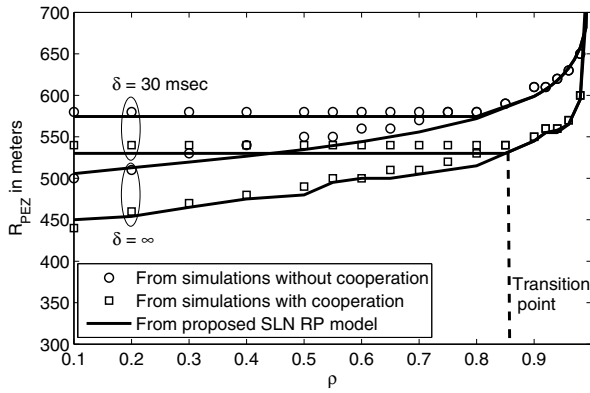


Fig. 9. Zoomed-in view of PEZ radius as a function of  $\rho$  using the SLN model with path-loss, shadowing, and Rayleigh fading for non-cooperative and cooperative SS ( $\Upsilon = 200$  CUs/km<sup>2</sup>,  $R_C = 100$  m, and  $I_{th} = -95$  dBm). The transition point shows the value of  $\rho$  below which the AED constraint is active.

and small-scale fading of the various links between the PU-Tx, PU-Rx, and CUs. We saw that the aggregate interference process is well characterized by SLN RP for moderate to high values of the interference, and we developed expressions for its CCDF, LCR, and autocorrelation. These led to expressions for its CCDF, LCR, and AED. We also saw how cooperative SS helps reduce the aggregate interference. Upon applying the model to PEZ design, we saw that a new constraint on the AED is often active, and should be accounted for. One interesting problem for future work is to characterize the aggregate interference in a more general scenario in which multiple PU-Txs communicate with multiple PU-Rxs.

## APPENDIX

### A. Derivation of Covariance Functions $C_Z(\tau)$ and $C_{I_\Sigma}(\tau)$

To obtain  $C_Z(\tau)$ , we match the covariance functions of  $I_\Sigma(t)$  and  $e^{Z(t)+s}$ . It can be easily shown that

$$C_{e^{Z(t)+s}}(\tau) = \mathbb{E} \left[ e^{Z(t)+Z(t+\tau)} \right] - \left( \mathbb{E} \left[ e^{Z(t)} \right] \right)^2. \quad (25)$$

From the expression for the moment generating function (MGF) of the jointly Gaussian RVs  $Z(t)$  and  $Z(t+\tau)$ , we get

$$C_{e^{Z(t)+s}}(\tau) = e^{2\mu_Z + \sigma_Z^2 + C_Z(\tau)} - e^{2\mu_Z + \sigma_Z^2}. \quad (26)$$

The covariance function  $C_{I_\Sigma}(\tau)$  of  $I_\Sigma(t)$  is given by

$$C_{I_\Sigma}(\tau) = \mathbb{E} \left[ \sum_{i=1}^{N_{CR}} I_i(t) \sum_{k=1, k \neq i}^{N_{CR}} I_k(t+\tau) \right] - \left( \mathbb{E} \left[ \sum_{i=1}^{N_{CR}} I_i(t) \right] \right)^2. \quad (27)$$

Conditioning over  $N_{CR}$  and evaluating the expectation over  $I_i(t)$  and  $I_i(t+\tau)$ , which are independent of  $N_{CR}$ , we get

$$C_{I_\Sigma}(\tau) = \mathbb{E}_{N_{CR}} \left[ \sum_{i=1}^{N_{CR}} \sum_{k=1, k \neq i}^{N_{CR}} \mathbb{E} [I_i(t)] \mathbb{E} [I_k(t+\tau)] \right. \\ \left. + \sum_{i=1}^{N_{CR}} \mathbb{E} [I_i(t)I_i(t+\tau)] \right] - \left( \mathbb{E}_{N_{CR}} \left[ \sum_{i=1}^{N_{CR}} \mathbb{E} [I_i(t)] \right] \right)^2. \quad (28)$$

Averaging over  $N_{CR}$ , we get

$$C_{I_\Sigma}(\tau) = \mathbb{E} [N_{CR} (N_{CR} - 1)] \mathbb{E} [I_i(t)] \mathbb{E} [I_k(t+\tau)] \\ + \mathbb{E} [N_{CR}] \mathbb{E} [I_i(t)I_i(t+\tau)] - \left( \mathbb{E} [N_{CR}] \mathbb{E} [I_i(t+\tau)] \right)^2. \quad (29)$$

Substituting  $\mathbb{E} [N_{CR}] = \Upsilon A$  and  $\mathbb{E} [N_{CR}^2] = \Upsilon A + (\Upsilon A)^2$ , where  $A = \pi (R^2 - R_{PEZ}^2)$ , we get

$$C_{I_\Sigma}(\tau) = \pi (R^2 - R_{PEZ}^2) \Upsilon \mathbb{E} [I_i(t)I_i(t+\tau)]. \quad (30)$$

Upon equating (26) and (30), we get (13).

### B. Non-cooperative SS: Derivation of $\mathbb{E} [I_i(t)^m]$ with Path-loss and Shadowing

Recall that the  $i^{\text{th}}$  CU transmits with power  $P_u$  if it detects the PU-Tx to be on, which happens with probability  $P_D(q(r_i(t), p, \cos \theta_i), Y_i, g_i))$ . Else, it transmits with power  $P_o$ . From the law of total probability and (5), we get

$$\mathbb{E} [I_i(t)^m] = \mathbb{E} \left[ \left( P_o K \left( \frac{d_0}{r_i(t)} \right)^\eta e^{\beta X_i(t)} \right)^m \right. \\ \left. \times (1 - P_D(q(r_i(t), p, \cos \theta_i), Y_i, g_i)) \right. \\ \left. + \left( P_u K \left( \frac{d_0}{r_i(t)} \right)^\eta e^{\beta X_i(t)} \right)^m P_D(q(r_i(t), p, \cos \theta_i), Y_i, g_i) \right)]. \quad (31)$$

Since  $X_i(t)$  is independent of the RVs  $r_i(t)$ ,  $\theta_i$ ,  $g_i$ , and  $Y_i$ , rearranging terms results in

$$\mathbb{E} [I_i(t)^m] = P_o^m K^m \mathbb{E} \left[ \left( \frac{d_0}{r_i(t)} \right)^{m\eta} \right] \mathbb{E} \left[ e^{m\beta X_i(t)} \right] \\ - (P_o^m - P_u^m) K^m \mathbb{E} \left[ e^{m\beta X_i(t)} \right] \\ \times \mathbb{E} \left[ \left( \frac{d_0}{r_i(t)} \right)^{m\eta} P_D(q(r_i(t), p, \cos \theta_i), Y_i, g_i) \right]. \quad (32)$$

Substituting the MGF of  $X_i(t)$  and the PDFs of  $Y_i$ ,  $g_i$ , and  $\theta_i$  (from (15)) in (32), we get

$$\mathbb{E} [I_i(t)^m] = P_o^m K^m e^{\frac{1}{2}m^2\beta^2\sigma_{sh}^2} \mathbb{E} \left[ \left( \frac{d_0}{r_i(t)} \right)^{m\eta} \right] \\ - (P_o^m - P_u^m) K^m e^{\frac{1}{2}m^2\beta^2\sigma_{sh}^2} \int_{-\infty}^{\infty} \frac{e^{-\frac{y_i^2}{2\sigma_{sh}^2}}}{\sigma_{sh}\sqrt{2\pi}} \int_0^{\infty} e^{-g_i} \int_0^{2\pi} \frac{1}{2\pi} \\ \times \mathbb{E} \left[ \left( \frac{d_0}{r_i(t)} \right)^{m\eta} P_D(q(r_i(t), p, \cos \theta_i), y_i, g_i) \right] dy_i dg_i d\theta_i. \quad (33)$$

Using Gauss-Hermite, Gauss-Laguerre, and Gauss-Chebyshev quadratures [19] to evaluate the integrals over  $y_i$ ,  $g_i$ , and  $\theta_i$ , respectively, yields

$$\mathbb{E} [I_i(t)^m] \approx P_o^m K^m e^{\frac{1}{2}m^2\beta^2\sigma_{sh}^2} \mathbb{E} \left[ \left( \frac{d_0}{r_i(t)} \right)^{m\eta} \right] \\ - \frac{1}{\sqrt{\pi}W_c} (P_o^m - P_u^m) K^m e^{\frac{1}{2}m^2\beta^2\sigma_{sh}^2} \\ \times \sum_{n_1=1}^{W_h} w_h(n_1) \sum_{n_2}^{W_l} w_l(n_2) \sum_{n_3=1}^{W_c} \mathbb{E} \left[ \left( \frac{d_0}{r_i(t)} \right)^{m\eta} \right. \\ \left. \times P_D(q(r_i(t), p, a_c(n_3)), \sqrt{2}\sigma_{sh}a_h(n_1), a_l(n_2)) \right]. \quad (34)$$

Given the total number of CUs, the location of the  $i^{\text{th}}$  CU is uniformly distributed over the region. Substituting the PDF of  $r_i(t)$  (from (15)) and simplifying yields (16).

### C. Non-cooperative SS: Derivation of $\mathbb{E}[I_i(t)I_i(t+\tau)]$ with Path-loss and Shadowing

Along lines similar to Appendix B, the autocorrelation of  $I_i(t)$  can be written as

$$\begin{aligned} \mathbb{E}[I_i(t)I_i(t+\tau)] &= P_o^2 K^2 \mathbb{E} \left[ e^{\beta(X_i(t)+X_i(t+\tau))} \right] \\ &\quad \times \mathbb{E} \left[ \left( \frac{d_0^2}{r_i(t)r_i(t+\tau)} \right)^\eta \right] \\ &\quad - (P_o^2 - P_u^2) K^2 \mathbb{E} \left[ e^{\beta(X_i(t)+X_i(t+\tau))} \right] \\ &\quad \times \mathbb{E} \left[ \left( \frac{d_0^2}{r_i(t)r_i(t+\tau)} \right)^\eta P_D(q(r_i(t), p, \cos \theta_i), Y_i, g_i) \right]. \end{aligned} \quad (35)$$

To simplify further, we assume that the distance  $r_i(t)$  between the CU and the PU-Rx is larger than the distance traveled by the CU in a time duration  $\tau$ :  $r_i(t+\tau) \approx r_i(t)$ . Else, the joint PDF of  $r_i(t)$  and  $r_i(t+\tau)$  needs to be taken into account. However, the time-variation of shadowing is accounted for. Rearranging terms and substituting the joint MGF of  $X_i(t)$  and  $X_i(t+\tau)$  (by using (3)), we get

$$\begin{aligned} \mathbb{E}[I_i(t)I_i(t+\tau)] &\approx P_o^2 K^2 e^{\beta^2 \sigma_{\text{sh}}^2 (1 + \exp(-\frac{v^2 \tau^2}{2D^2}))} \\ &\quad \times \mathbb{E} \left[ \frac{d_0^{2\eta}}{r_i(t)^{2\eta}} \right] - (P_o^2 - P_u^2) K^2 e^{\beta^2 \sigma_{\text{sh}}^2 (1 + \exp(-\frac{v^2 \tau^2}{2D^2}))} \\ &\quad \times \mathbb{E} \left[ \left( \frac{d_0}{r_i(t)} \right)^{2\eta} P_D(q(r_i(t), p, \cos \theta_i), Y_i, g_i) \right]. \end{aligned} \quad (36)$$

Averaging over the RVs  $Y_i$ ,  $g_i$ , and  $\theta_i$ , as in Appendix B, we get

$$\begin{aligned} \mathbb{E}[I_i(t)I_i(t+\tau)] &\approx P_o^2 K^2 e^{\beta^2 \sigma_{\text{sh}}^2 (1 + \exp(-\frac{v^2 \tau^2}{2D^2}))} \\ &\quad \times \mathbb{E} \left[ \frac{d_0^{2\eta}}{r_i(t)^{2\eta}} \right] - \frac{(P_o^2 - P_u^2) K^2}{\sqrt{\pi} W_c} e^{\beta^2 \sigma_{\text{sh}}^2 (1 + \exp(-\frac{v^2 \tau^2}{2D^2}))} \\ &\quad \times \sum_{n_1=1}^{W_h} w_h(n_1) \sum_{n_2=1}^{W_l} w_l(n_2) \sum_{n_3=1}^{W_c} \mathbb{E} \left[ \left( \frac{d_0}{r_i(t)} \right)^{2\eta} \right. \\ &\quad \left. \times P_D(q(r_i(t), p, a_c(n_3)), \sqrt{2} \sigma_{\text{sh}} a_h(n_1), a_l(n_2)) \right]. \end{aligned} \quad (37)$$

Substituting the PDF of  $r_i(t)$ , which is given in (15), and simplifying yields (17).

### D. Cooperative SS: With Path-loss and Shadowing

1) *Derivation of  $\mathbb{E}[I_i(t)^m]$* : The probability of detection by a CU with cooperative SS depends on the SNRs of all its cooperating CUs, which are within a radius  $R_C$  from it. Let  $M$  be the number of cooperating CUs and let  $\Gamma = [\gamma_1, \gamma_2, \dots, \gamma_M]$  denote their SNRs. Then, the probability of

detection  $P_{\text{D,OR}}^{(i)}(\Gamma)$  of the  $i^{\text{th}}$  CU using the OR fusion rule is given by [18]

$$P_{\text{D,OR}}^{(i)}(\Gamma) = 1 - (1 - P_{\text{Di}}) \prod_{k=1, k \neq i}^M (1 - P_{\text{Dj}}), \quad (38)$$

where

$$\begin{aligned} P_{\text{Di}} &= P_D(q(r_i(t), p, \cos \theta_i), Y_i, g_i), \\ P_{\text{Dj}} &= P_D(q(r_{ij}(t), q(r_i(t), p, \cos \theta_i), \cos \theta_{ij}), Y_j, g_j), \quad k \neq i, \end{aligned} \quad (39)$$

And, neglecting boundary effects,  $M$  is a Poisson RV with mean  $\Upsilon \pi R_C^2$ .

Proceeding along lines similar to Appendix B, the  $m^{\text{th}}$  moment of  $I_i(t)$  is given by

$$\begin{aligned} \mathbb{E}[I_i(t)^m] &\approx P_o^m K^m e^{\frac{1}{2} m^2 \beta^2 \sigma_{\text{sh}}^2} \mathbb{E} \left[ \left( \frac{d_0}{r_i(t)} \right)^{m\eta} \right] \\ &\quad - (P_o^m - P_u^m) K^m e^{\frac{1}{2} m^2 \beta^2 \sigma_{\text{sh}}^2} \\ &\quad \times \mathbb{E} \left[ \left( \frac{d_0}{r_i(t)} \right)^{m\eta} \left( 1 - (1 - P_{\text{Di}}) \prod_{k=1, k \neq i}^M (1 - P_{\text{Dj}}) \right) \right]. \end{aligned} \quad (41)$$

Conditioning on the position of the  $i^{\text{th}}$  CU and  $M$ , the second expectation term above becomes

$$\begin{aligned} &\mathbb{E} \left[ \left( \frac{d_0}{r_i(t)} \right)^{m\eta} \left( 1 - (1 - P_{\text{Di}}) \prod_{k=1, k \neq i}^M (1 - P_{\text{Dj}}) \right) \right] \\ &= \mathbb{E}_{r_i(t), \theta_i} \left[ \left( \frac{d_0}{r_i(t)} \right)^{m\eta} \right. \\ &\quad \left. \times \left( 1 - (1 - \mathbb{E}[P_{\text{Di}}]) \mathbb{E}_M \left[ (1 - \mathbb{E}[P_{\text{Dj}}])^{M-1} \right] \right) \right], \end{aligned} \quad (42)$$

where

$$\begin{aligned} \mathbb{E}[P_{\text{Di}}] &\triangleq f_1(r_i(t), \cos \theta_i) = \int_{-\infty}^{\infty} \frac{e^{-\frac{y_i^2}{2\sigma_{\text{sh}}^2}}}{\sigma_{\text{sh}} \sqrt{2\pi}} \\ &\quad \times \int_0^{\infty} e^{-g_i} P_D(q(r_i, p, \theta_i), y_i, g_i) dg_i dy_i, \end{aligned} \quad (43)$$

$$\begin{aligned} \mathbb{E}[P_{\text{Dj}}] &\triangleq f_2(r_i(t), \cos \theta_i) = \int_{-\infty}^{\infty} \frac{e^{-\frac{y_j^2}{2\sigma_{\text{sh}}^2}}}{\sigma_{\text{sh}} \sqrt{2\pi}} \int_0^{\infty} e^{-g_j} \\ &\quad \times \int_0^{2\pi} \int_0^{R_C} \frac{r_{ij}}{\pi R_C^2} P_D(q(r_{ij}, q(r_i(t), p, \cos \theta_i), \cos \theta_{ij}), y_j, g_j) \\ &\quad \times dr_{ij} d\theta_{ij} dg_j dy_j. \end{aligned} \quad (44)$$

As in Appendix B, after using Gauss quadrature to evaluate the above integrals, the expressions for  $f_1$  and  $f_2$  simplify to (22) and (23), respectively. Substituting (42) in (41) and averaging over  $\theta_i$ ,  $r_i(t)$ , and  $M$  yields (21).

2) *Derivation of  $\mathbb{E}[I_i(t)I_i(t+\tau)]$* : Along lines similar to Appendices B and C, the autocorrelation of  $I_i(t)$  can be

written as

$$\begin{aligned} \mathbb{E}[I_i(t)I_i(t+\tau)] &= P_o^2 K^2 e^{\beta^2 \sigma_{sh}^2 \left(1 + \exp\left(\frac{-v^2 \tau^2}{2D^2}\right)\right)} \\ &\times \mathbb{E}\left[\left(\frac{d_0}{r_i(t)}\right)^{2\eta}\right] - (P_o^2 - P_u^2) K^2 e^{\beta^2 \sigma_{sh}^2 \left(1 + \exp\left(\frac{-v^2 \tau^2}{2D^2}\right)\right)} \\ &\times \mathbb{E}\left[\left(\frac{d_0}{r_i(t)}\right)^{2\eta} P_{D,OR}^{(i)}(\Gamma)\right]. \quad (45) \end{aligned}$$

Simplifying further, we get (24).

## REFERENCES

- [1] M. Win, P. Pinto, and L. Shepp, "A mathematical theory of network interference and its applications," *Proc. IEEE*, vol. 97, no. 2, pp. 205–230, Feb. 2009.
- [2] A. Rabbachin, T. Q. S. Quek, H. Shin, and M. Z. Win, "Cognitive network interference," *IEEE J. Sel. Areas Commun.*, vol. 29, no. 2, pp. 480–493, Feb. 2011.
- [3] A. Ghasemi and E. S. Sousa, "Interference aggregation in spectrum-sensing cognitive wireless networks," *IEEE J. Sel. Topics Signal Process.*, vol. 2, no. 1, pp. 41–56, Feb. 2008.
- [4] Z. Chen, C.-X. Wang, X. Hong, J. S. Thompson, S. A. Vorobyov, X. Ge, H. Xiao, and F. Zhao, "Aggregate interference modeling in cognitive radio networks with power and contention control," *IEEE Trans. Commun.*, vol. 60, no. 2, pp. 456–468, Feb. 2012.
- [5] M. Hanif, M. Shafi, P. Smith, and P. Dmochowski, "Interference and deployment issues for cognitive radio systems in shadowing environments," in *Proc. 2009 ICC*, pp. 1–6.
- [6] M. Hanif and P. Smith, "On the statistics of cognitive radio capacity in shadowing and fast fading environments," *IEEE Trans. Wireless Commun.*, vol. 9, no. 2, pp. 844–852, Feb. 2010.
- [7] G. Stuber, S. Almfouh, and D. Sale, "Interference analysis of TV-band whitespace," *Proc. IEEE*, vol. 97, no. 4, pp. 741–754, Apr. 2009.
- [8] P. Talmola, J. Kalliovaara, J. Paavola, R. Ekman, A. Vainisto, N. Aurala, H. Kokkinen, K. Heiska, R. Wichman, and J. Poikonen, "Field measurements of WSD-DTT protection ratios over outdoor and indoor reference geometries," in *Proc. 2012 CROWNCOM*, pp. 7–12.
- [9] A. Ben Hadj Alaya-Feki, B. Sayrac, S. Ben Jemaa, and E. Moulines, "Interference cartography for hierarchical dynamic spectrum access," in *Proc. 2008 DySPAN*, pp. 1–5.
- [10] A. Goldsmith, S. A. Jafar, I. Maric, and S. Srinivasa, "Breaking spectrum gridlock with cognitive radios: an information theoretic perspective," *Proc. IEEE*, vol. 97, no. 5, pp. 894–914, May 2009.
- [11] G. L. Stüber, *Principles of Mobile Communication*, 2nd ed. Springer, 2011.
- [12] M. Vu, N. Devroye, and V. Tarokh, "On the primary exclusive region of cognitive networks," *IEEE Trans. Wireless Commun.*, vol. 8, no. 7, pp. 3380–3385, July 2009.
- [13] A. Bagayoko, P. Tortelier, and I. Fijalkow, "Impact of shadowing on the primary exclusive region in cognitive networks," in *Proc. 2010 Eur. Wireless Conf.*, pp. 105–110.
- [14] J. J. Lehtomaki, "Performance comparison of multichannel energy detector output processing methods," in *Proc. 2003 Int. Symp. Signal Process. App.*, pp. 261–264.
- [15] J. Lai and N. Mandayam, "Minimum duration outages in Rayleigh fading channels," *IEEE Trans. Commun.*, vol. 49, no. 10, pp. 1755–1761, Oct. 2001.
- [16] P. Smith, H. Suraweera, and M. Shafi, "Signal power variation with applications to cognitive radio," in *Proc. 2008 Commun. Theory Workshop*, pp. 33–38.
- [17] M. Hanif and P. Smith, "Level crossing rates of interference in cognitive radio networks," *IEEE Trans. Wireless Commun.*, vol. 9, no. 4, pp. 1283–1287, Apr. 2010.
- [18] E. Peh and Y.-C. Liang, "Optimization for cooperative sensing in cognitive radio networks," in *Proc. 2007 WCNC*, pp. 27–32.
- [19] M. Abramowitz and I. Stegun, *Handbook of Mathematical Functions with Formulas, Graphs, and Mathematical Tables*, 9th ed. Dover, 1972.
- [20] A. Sonnenschein and P. M. Fishman, "Radiometric detection of spread-spectrum signals in noise of uncertain power," *IEEE Trans. Aerosp. Electron. Syst.*, vol. 28, no. 3, pp. 654–660, July 1992.
- [21] M. Wildemeersch, T. Q. S. Quek, A. Rabbachin, C. H. Slump, and A. Huang, "Energy efficient design of cognitive small cells," in *Proc. 2013 ICC*, pp. 1294–1299.
- [22] T. Yucek and H. Arslan, "A survey of spectrum sensing algorithms for cognitive radio applications," *IEEE Commun. Surv. Tuts.*, vol. 11, no. 1, pp. 116–130, Mar. 2009.
- [23] S. Karlin and H. E. Taylor, *A First Course in Stochastic Processes*, 2nd ed. Academic Press, Inc. Ltd., 1975.
- [24] G. Bianchi, "Performance analysis of the IEEE 802.11 distributed coordination function," *IEEE J. Sel. Areas Commun.*, vol. 18, no. 3, pp. 535–547, Sept. 2006.
- [25] N. C. Beaulieu, A. A. Abu-Dayya, and P. J. McLane, "Estimating the distribution of a sum of independent lognormal random variables," *IEEE Trans. Commun.*, vol. 43, no. 12, pp. 2869–2873, Dec. 1995.
- [26] N. B. Mehta, J. Wu, A. F. Molisch, and J. Zhang, "Approximating a sum of random variables with a lognormal," *IEEE Trans. Wireless Commun.*, vol. 6, no. 7, pp. 2690–2699, July 2007.
- [27] C. Fischione, F. Graziosi, and F. Santucci, "Approximation for a sum of on-off lognormal processes with wireless applications," *IEEE Trans. Commun.*, vol. 55, no. 10, pp. 1984–1993, Oct. 2007.
- [28] I. A. Koutrouvelis, "Regression-type estimation of the parameters of stable laws," *Amer. Stat. Assoc.*, vol. 75, no. 372, pp. 918–928, Dec. 1980.
- [29] M. F. Hanif, N. C. Beaulieu, and D. J. Young, "Two useful bounds related to weighted sums of Rayleigh random variables with applications to interference systems," *IEEE Trans. Commun.*, vol. 60, no. 7, pp. 1788–1792, July 2012.
- [30] R. Barakat, "Sums of independent lognormally distributed random variables," *J. Opt. Soc. Amer.*, vol. 66, no. 3, pp. 211–216, Mar. 1976.



**Mohd. Shabbir Ali** received his Bachelor of Engineering degree in Electrical and Electronics Eng. from the MuffakhamJah College of Eng. and Technology (MJCT), Hyderabad, India in 2010. He is an M.Sc. (Eng.) student in the Dept. of Electrical Communication at the Indian Institute of Science (IISc), Bangalore. His research interests include cognitive radio networks, homogeneous and heterogeneous networks, and interference modeling and management.



**Neelesh B. Mehta** (S'98-M'01-SM'06) received his Bachelor of Technology degree in Electronics and Communications Eng. from the Indian Institute of Technology (IIT), Madras in 1996, and his M.S. and Ph.D. degrees in Electrical Eng. from the California Institute of Technology, Pasadena, USA in 1997 and 2001, respectively. He is now an Associate Professor in the Dept. of Electrical Communication Eng., Indian Institute of Science (IISc), Bangalore. Before joining IISc in 2007, he was a research scientist in USA from 2001 to 2007 in AT&T Laboratories, NJ, Broadcom Corp., NJ, and Mitsubishi Electric Research Laboratories (MERL), MA.

His research includes work on link adaptation, multiple access protocols, cellular systems, MIMO and antenna selection, cooperative communications, energy harvesting networks, and cognitive radio. He was also actively involved in the Radio Access Network (RAN1) standardization activities in 3GPP from 2003 to 2007. He has co-authored 45+ IEEE transactions papers, 70 conference papers, and 3 book chapters, and is a co-inventor in 20 issued US patents. He has served as a TPC co-chair for tracks/symposia in COMSNETS 2014, Globecom 2013, ICC 2013, WISARD 2010 and 2011, NCC 2011, VTC 2009 (Fall), and Chinacom 2008. He is an Editor of IEEE WIRELESS COMMUNICATIONS LETTERS, IEEE TRANSACTIONS ON COMMUNICATIONS, and the *Journal of Communications and Networks*. He currently serves as the Director of Conference Publications on the Board of Governors of IEEE ComSoc.